On entropic barriers for diffusion in zeolites: A molecular dynamics study

Andreas Schüring
Universität Leipzig, Institut für Theoretische Physik, Augustusplatz 10-11, D–04109 Leipzig, Germany

Scott M. Auerbach
Department of Chemistry and Department of Chemical Engineering, University of Massachusettes, Amherst, Massachusetts 01003

Siegfried Fritzsche and Reinhold Haberlandt
Universität Leipzig, Institut für Theoretische Physik, Augustusplatz 10-11, D–04109 Leipzig, Germany

(Received 7 November 2001; accepted 28 March 2002)

The self-diffusion of ethane in cation-free Linde type A zeolite has been studied by molecular dynamics simulations for various temperatures. These simulations predict that the diffusivity *decreases* with increasing temperature between 150 K and 300 K for a low loading of one molecule per cage. The rate of cage-to-cage crossings shows the same temperature dependence. We explain this phenomenon based on an analysis of the activation entropy that controls motion through eight-ring windows separating adjacent cages. The diffusivity and the cage-to-cage rate constant both decrease with temperature because heating the system moves ethane away from eight-ring windows, on average, which increases the entropic barrier for cage-to-cage motion. © *2002 American Institute of Physics.* [DOI: 10.1063/1.1480011]

I. INTRODUCTION

Zeolites[1] have outstanding properties due to their regular microporous structures and high internal surface areas. They are used in manifold industrial processes such as catalysts and sorbents with high shape selectivities,[2] which result from strong host–guest interactions. This fact has led to growing interest in modeling the transport of molecules in zeolites.[3]

In many cases, self-diffusivities can be expressed as $D_S = k_{hop} a^2$, where k_{hop} is a site-to-site rate constant and a is an average site-to-site distance. According to transition state theory[4] (TST), we can express k_{hop} as

$$k_{hop}^{TST} = \left[\frac{\omega(T)}{2\pi} e^{\Delta S(T)/k_B} \right] e^{-\beta \Delta E(T)}, \tag{1}$$

where T is the temperature, k_B is Boltzmann's constant, $\beta = 1/k_B T$, $\omega(T)$ is the temperature-dependent site vibrational frequency, $\Delta S(T)$ is the temperature-dependent activation entropy, and $\Delta E(T)$ is the temperature-dependent activation energy. When considering a broad temperature range including temperatures for which $\beta \Delta E(T) \gg 1$, the Boltzmann factor in Eq. (1) dominates the temperature dependence of k_{hop}, rendering the factor in square brackets an apparent preexponential constant usually denoted by the apparent frequency ν. In this case self-diffusivities exhibit an Arrhenius temperature dependence taking the form $D_\infty e^{-\beta E_a}$, where $D_\infty = \nu a^2$ and E_a is an apparent activation energy. In some cases, this activation energy corresponds to a potential energy barrier characterizing a site-to-site jump; in other cases, the apparent activation energy represents a composite of several fundamental energy scales.[5] Because the Arrhenius temperature dependence is so common, we have come to expect that diffusivities increase with temperature for *all* host–guest systems.

However, when considering temperatures for which $\beta \Delta E(T) \lesssim 1$, the temperature dependence of the preexponential factor can become important. Temperature dependencies associated with activation entropies can be much more unusual than the Arrhenius dependence, and can even produce nonmonotonic temperature dependencies. In this article, we explore such phenomena by modeling ethane diffusion in Linde type A[1] (LTA) zeolite using both molecular dynamics and window sampling methods. We find that the diffusivity *decreases* with increasing temperature between 150 K and 300 K for a low loading of one molecule per cage. We explain this phenomenon based on an analysis of the activation entropy that controls motion through eight-ring windows separating adjacent cages.

The remainder of this paper is organized as follows: in Sec. II we discuss the model of ethane in LTA zeolite; in Sec. III we describe the window sampling of internal and free energies; in Sec. IV we discuss the molecular dynamics (MD) and window sampling results; and in Sec. V we give concluding remarks.

II. MODEL OF THE HOST–GUEST SYSTEM

Ethane was modeled in the "united atom" approximation[6] with two interaction sites. Lennard-Jones potentials were assumed between the sites so that the potential energy between two molecules A and B is given as

$$V_{AB} = \sum_{i=1}^{2} \sum_{j=1}^{2} 4\epsilon \left[\left(\frac{\sigma}{r_{ij}} \right)^{12} - \left(\frac{\sigma}{r_{ij}} \right)^{6} \right], \tag{2}$$

where i and j number sites of molecule A and B, respectively. The intermolecular potential parameters were taken from Ref. 7 and are listed in Table I. A Morse potential

$$V(r) = D[1 - e^{-\beta(r - r_0)}]^2 \tag{3}$$

TABLE I. Lennard-Jones potential parameters.

	σ (Å)	ϵ (kJ/mol)
CH_3-CH_3	3.78	0.866
CH_3-O	3.17	1.18
CH_3-Si	2.12	0.683

with $D=83.9$ kJ/mol, $\beta=1.84$ Å^{-1}, and $r_0=1.54$ Å as in Ref. 8 was assumed between the two sites of a molecule to include molecular vibrations into the model. For the vibrations of the zeolite lattice the spring force model of Demontis and co-workers[9,10] was used. Therein harmonic potentials are chosen between tetrahedrally coordinated atoms (T-atoms) and O-atoms and furthermore between O atoms bound to the same T atom in order to achieve the tetrahedral arrangement of the oxygen atoms around the T atoms. The equilibrium distances were taken from the structural data supplied in Ref. 11. The guest–host interaction is described by Lennard-Jones potentials. The Lennard-Jones parameters for oxygen taken from Ref. 12 were combined with the above-mentioned intermolecular parameters using the rules of Lorentz-Berthelot

$$\sigma_{12}=(\sigma_1+\sigma_2)/2, \quad \epsilon_{12}=\sqrt{\epsilon_1\epsilon_2} \tag{4}$$

(see Table I). The shifted force simulation technique[6] has been employed for all Lennard-Jones interactions. The cutoff radii were chosen to be 2.5σ of the respective interaction.

III. WINDOW SAMPLING METHODS

To understand the temperature dependence of self-diffusivities calculated from mean-square displacements, we analyze the dynamics in the language of cage-to-cage jumps.[4] The cubic symmetry of LTA zeolite (see Fig. 1) allows us to write $D_S=\frac{1}{6}k_{cage}a^2$, where the factor of $\frac{1}{6}$ arises from three dimensions, a is the root-mean-square jump distance, and $1/k_{cage}$ is the mean cage lifetime. The cage-to-cage rate constant can be estimated by noting that $k_{cage}=6k_{hop}$, where k_{hop} is a fundamental rate constant for hopping through an eight-ring window separating adjacent LTA α cages. We can then estimate k_{hop} from transition state theory by calculating the free energy surface along a cage-to-cage coordinate, denoted in this case by x. Because of the cubic symmetry, either x, y, or z suffices. To analyze the cage-to-cage dynamics, in addition to simply calculating the relevant rate constants, we also need to compute the local thermodynamic internal energy. Thus, we discuss below window sampling methods for calculating the local Helmholtz free energy, $A(x)$, as well as the local internal energy, $U(x)$.

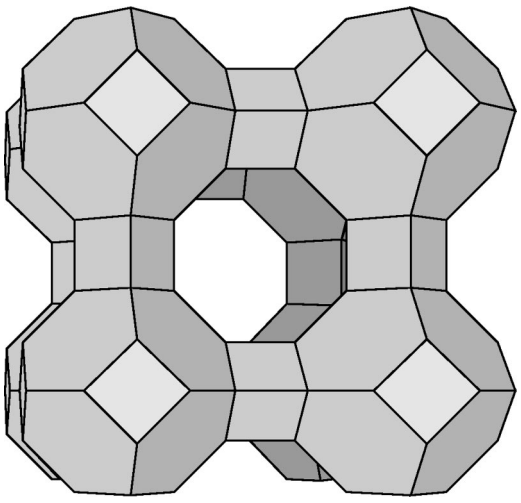

FIG. 1. Structure scheme of LTA zeolites. The vertices mark the positions of the T atoms; the lines symbolize the oxygen bridges between them. The edges of the cube shown are formed by sodalite units consisting of four and six rings. The sodalite units surround the large α cage of ≈ 1 nm diameter. The eight rings, which are often called windows, have a free diameter of ≈ 0.41 nm. They build the connection between the cages and can be passed by small hydrocarbons such as ethane.

In terms of the Helmholtz free energy, the transition state theory (TST) rate constant is given by

$$k_{hop}^{TST}=(2\pi\beta m)^{-1/2}\frac{\exp\{-\beta A(x^{\ddagger})\}}{\int_{reac} dx\,\exp\{-\beta A(x)\}}, \tag{5}$$

where m is the particle mass, $x^{\ddagger}$ is the x coordinate of the transition state, and "reac" signifies the reactant region of configuration space. The local Helmholtz free energy, $A(x)$, is defined by

$$\frac{e^{-\beta A(x_0)}}{L}\equiv\langle\delta(x-x_0)\rangle, \tag{6}$$

where L is a length scale necessary for definition but not for computation, $\delta(x)$ is the Dirac delta function, and the average $\langle\cdots\rangle$ is carried out in the canonical ensemble. Applying the fact that

$$n(x)\propto\exp\{-\beta A(x)\} \tag{7}$$

allows the TST rate constant to be calculated from the one-particle density distribution $n(x)$. For simplicity, $n(x)$ shall be normalized according to $\int_{cage}n(x)dx=1$. $n(x)$ can be easily evaluated during molecular dynamics simulations counting the number $N(x_i)$ of molecules appearing between two positions x_i and $x_i+\Delta x$ in a histogram. Then

$$n(x)=\frac{1}{\Delta x}\frac{N(x_i)}{\sum_i N(x_i)} \tag{8}$$

holds and Eq. (5) becomes

$$k_{hop}^{TST}\approx(2\pi\beta m)^{-1/2}\frac{n(x^{\ddagger})}{1-\Delta x n(x^{\ddagger})}. \tag{9}$$

In practice, we use histograms with 123 bins of $\Delta x=0.1$ Å width in each LTA cage to compute both $A(x)$ and the local internal energy $U(x)$; the latter is averaged per bin. 5×10^6 time steps are required to converge these averages to sufficient precision.

IV. RESULTS AND DISCUSSION

The self-diffusion coefficients were calculated from the slope of the mean-square displacement of the molecules via the Einstein equation

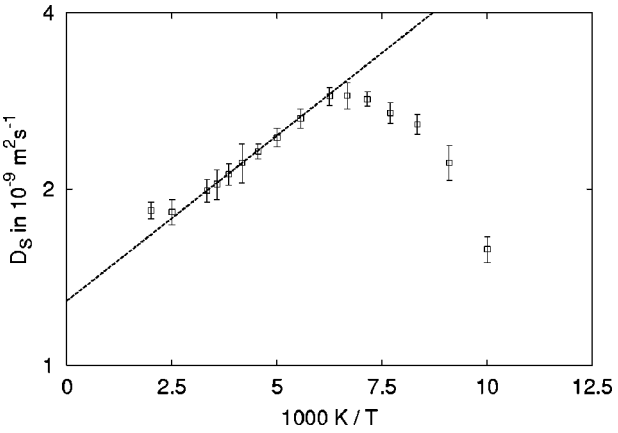

FIG. 2. Arrhenius diagram for D_S at a loading of one ethane molecule per cage. Between $T=150$ K and 400 K the Arrhenius law can be fitted with $E_A=-1.1$ kJ/mol.

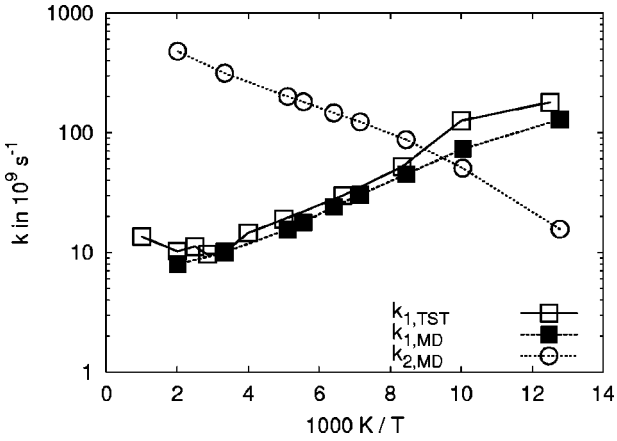

FIG. 3. Intercage jump rate k_1 and intracage jump rate k_2 evaluated from the particle trajectories (subscript MD), and k_1 obtained from transition state theory (subscript TST).

$$D_S=\frac{d}{dt}\frac{\langle \Delta \vec{r}^2\rangle}{6}. \tag{10}$$

The validity of the diffusion equation was checked via the momentum method.[13] The hydrodynamic limit, i.e., when the propagator is a Gaussian in sufficient approximation, was found to be reached after a time $\langle\tau\rangle$ given as the mean residence time in the cage

$$\langle\tau\rangle=a^2/6D_S, \tag{11}$$

where $a=1.23$ nm is the cage-to-cage distance. Therefore D_S was evaluated from the slope of the mean-square displacement in an interval of approximately $\langle\tau\rangle$ to $4\langle\tau\rangle$. The statistical error for D_S was estimated by evaluating four parts of the trajectory. Each part had a length of 25 ns, which is approximately 100 times the residence time $\langle\tau\rangle$ when $D_S=10^{-9}$ m^2/s. Thus independence of the parts can well be assumed. The standard deviations for the D_S range between 5% and 10% of the corresponding average values. We repeated the simulations with different starting configurations for some temperatures and found agreement with the first calculations indicating that the statistical accuracy is sufficient.

The simulation results for the self-diffusion coefficients at a low loading of one ethane molecule per cage are plotted in Fig. 2 in a logarithmic scale over the inverse temperature. A complex temperature dependence is observed. In the low-temperature region below $T=130$ K D_S increases strongly with T. Between 130 K and 150 K the temperature dependence shows a crossover between an increase and a decrease with increasing T. The maximum value of $D_S=2.9\times10^{-9}$ m^2/s is found at $T\approx150$ K. Between $T=150$ K and 300 K the Arrhenius law

$$D_S(T)=D_\infty \exp\{-\beta E_A\} \tag{12}$$

can be fitted, but with a negative temperature coefficient $E_A=-1.1$ kJ/mol (the preexponential factor is $D_\infty=1.3\times10^{-9}$ m^2/s). Although negative activation energies have been seen for other systems, e.g., electron transfer in biological systems, the physics of this zeolite–guest system is probably too simple to admit such behavior. As such we seek an alternative explanation.

As a first step we checked for the preferred positions of the molecules within the cage and the jumps of the molecules between them. The particle density $n(x)$ has local maxima in front of the windows for $T>100$ K. Therefore we defined spherical volumes around the maxima of $n(x)$ as adsorption sites in the cage. A radius of the spheres of 2 Å and the distance of the sphere centers from the dividing surface between adjacent cages of 2.15 Å were suitable values for the evaluation of the jumps. Two kinds of jumps are distinguished:

(1) jumps through the window into another cage and
(2) jumps within the same cage.

The first kind will be referred to as *intercage* jumps with the according jump rate k_1, the second kind will be referred to as *intracage* jumps with the according jump rate k_2. The results of this evaluation are plotted in an Arrhenius diagram in Fig. 3. k_1 decreases with increasing temperature over the whole examined range of temperatures. The temperature coefficient of the Arrhenius law was fitted to $E_A=-2.6$ kJ/mol, which is even lower than the value observed for the self-diffusion coefficients. In contrast, k_2 shows normal Arrhenius temperature dependence with a positive value of $E_A=2.1$ kJ/mol. It can be seen that k_2 is lower than k_1 below $T=100$ K and vice versa. The rule that the lowest rate limits the self-diffusion coefficient can be applied here to describe the temperature dependence of D_S. The reason for this lies in the topology of the site distribution. On their diffusion path the molecules have to jump inside the cage from one window region to another; otherwise there was an infinite chain of jumps between two cages through the connecting window. We are currently developing a jump model to combine the jump rates k_1 and k_2 with the self-diffusion coefficient D_S.

As a second step we apply transition state theory to calculate the rate k_1 of cage-to-cage jumps and to evaluate the activation entropy. $k_{\mathrm{hop}}^{\mathrm{TST}}$ is calculated from Eq. (9). For the overall cage-to-cage jump rate,

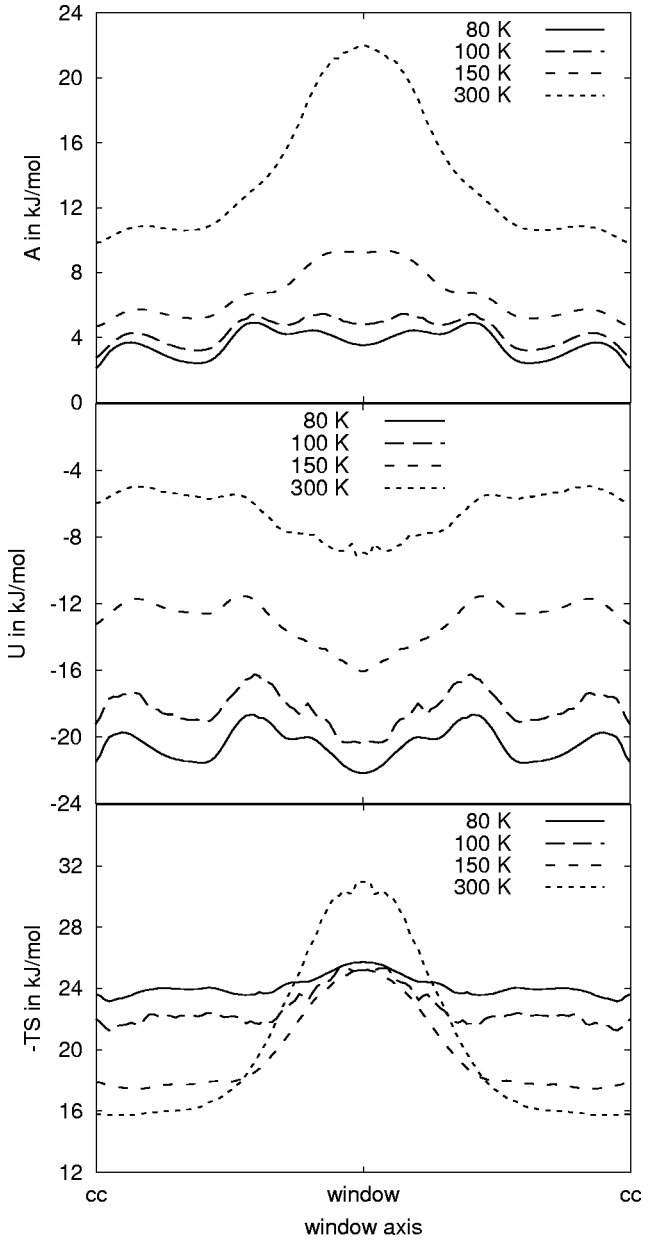

FIG. 4. Free energy, internal energy, and entropy of the molecule along an axis from the center of one cage to another cage for different temperatures. The centers of the cages are labeled by cc.

$$k_1^{\mathrm{TST}} = 6k_{\mathrm{hop}}^{\mathrm{TST}} \tag{13}$$

holds, as there are six equivalent ways (windows) to leave the cage. The resulting rates k_1^{TST} are also shown in Fig. 3. The temperature dependence is not simply of Arrhenius type, but there is good agreement with the rates k_1^{MD} evaluated from the trajectories. The TST values are slightly higher as there is a finite gap between the volumes on the two sides of a window so that some oscillations are not counted.

The entropy calculation also requires the internal energy $U(x)=K(x)+V(x)$ to obtain $-TS(x)=A(x)-U(x)$. The three quantities are plotted in Fig. 4 for different temperatures. At 80 K, the profile of the local Helmholtz free energy $A(x)$ is similar to the profile of the internal energy $U(x)$ with a local minimum at the position of the window. At this low temperature $-TS(x)$ is nearly independent of space. On increasing the temperature, $A(x)$ becomes more dominated by the entropy contribution $-TS(x)$. $-TS(x)$ shows a local maximum that increases with temperature at the position of the window. At temperatures of 150 K and higher, the entropy contribution leads to a local maximum of $A(x)$ in the window. These results indicate that the anomalous temperature dependencies of the cage-to-cage rate and the self-diffusion coefficient are based on an effect of the entropy.

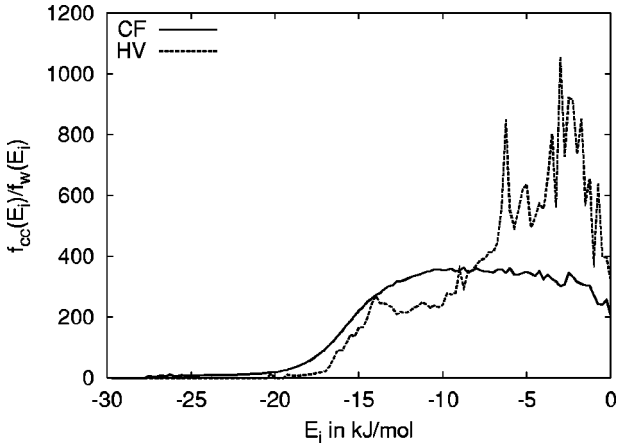

FIG. 5. Ratio of the numbers of isoenergetic configurations (label CF) in the cage center (cc) and the window (w). The curve labeled by HV is obtained from the averaging of E in small hypervolumes; see text.

At 300 K the entropic barrier is 15 kJ/mol. While this is a plausible result, we seek to understand the origin of this significant entropy barrier. Towards that end, we computed the distribution $f_j(E)$ of energy levels in the window (index $j=w$) and the cage center bin (index $j=\mathrm{cc}$). The statistics counted at temperature T in bins with an energy $E_i<E<E_i+\Delta E$ ($\Delta E=0.25$ kJ/mol) are denoted as $N_j(E_i)$, and N is the total number of counts in the simulation for all molecules. Defining the degeneracy function $f_j(E_i)$ according to

$$N_j(E_i)/N \equiv f_j(E_i)\exp\{-\beta E_i\}, \tag{14}$$

$f_j(E_i)$ should thus be independent of temperature and simulation time (provided this time is sufficiently long). The statistical thermodynamic interpretation of $f_j(E_i)$ via the Boltzmann entropy formula yields the entropy $S_j(E_i)=k_B \ln f_j(E_i)$. The entropy barrier found above is then consistent with the ratio $f_{\mathrm{cc}}(E_i)/f_w(E_i)\cong 400$. This ratio, obtained by evaluating the configurations occurring during the simulation, is plotted with the label CF in Fig. 5 as a function of the system potential energy, E_i. The resulting degeneracy ratios for energies above -15 kJ/mol fall in the range of 300–400, in excellent agreement with the entropy barrier discussed above.

These large factors can be understood by analyzing molecular translation and rotational degrees of freedom. We divided the cage-center and window bins into hypervolumes of 0.01 nm in y and z directions, as well as another 20×20 array for the orientations. The fraction of hypervolumes with an average energy E in the cage-center bin, compared to the window bin, is plotted in Fig. 5 labeled by HV. Regardless of the fact that, due to the averaging of E, the results do not

exactly coincide, the order of magnitude is reproduced. We find that the geometry of the window allows molecular access in the window bin to a range of ≈ 10 bins in y and z directions, to 4 bins in $\cos\theta$ and to all 20 bins in ϕ (totaling ≈ 6500 hypervolumes visited). In the cage center, rotation is less restricted the larger the distance to the cage walls. Thus, the large factor between the number of hypervolumes of equal energy can be explained by the larger area in the y and z directions and additionally by the hindrance of rotations in the window.

V. CONCLUDING REMARKS

We have reported results from MD simulations of the self-diffusion of ethane in cation-free LTA zeolite at a low loading of one molecule per cage. The temperature dependence of the self-diffusion coefficient shows a decrease with increasing temperature between 150 K and 300 K. The same temperature dependence is found for the rate k_{cage} of cage-to-cage crossings. An explanation for the effect was found in the activation entropy of k_{cage}. On increasing the temperature, the molecules explore more and more of the cage volume leading to a decreased probability of finding a molecule in the window connecting adjacent cages. The significant height of the entropic barrier at 300 K was shown to result from the high number of isoenergetic configurations due to the larger freedom for translation as well as for rotation in the cage center compared to the window.

We expect entropic barriers to appear relatively often in zeolite–sorbate systems. If energetic barriers are high, these entropic barriers serve only to modulate the magnitudes of apparent preexponential factors. But when energetic barriers are relatively small, these entropic barriers can produce rather exotic temperature dependencies, as seen above. The negative activation energies for cage-to-cage rates observed by Yashonath and co-workers for spherical molecules in A- and Y-type zeolites[14–16] might arise from the same activation entropies observed in the present study. According to our results, the entropic barrier is expected to be lower in the case of spherical molecules. Nevertheless, the temperature coefficients E_a are in the same order of magnitude. In the mentioned papers[14–16] no decrease of the self-diffusion coefficient with increasing temperature has been reported. One can assume that in these cases the rate governed by the entropy was not the diffusion-limiting rate.

In future work, we are developing a jump diffusion model to relate the intra- and intercage rate constants with the self-diffusion constant. We are also searching for an existing cation-free zeolite with which to test experimentally the predictions made herein.

ACKNOWLEDGMENTS

The authors thank Professor Troe (Göttingen), Professor Kärger, Professor Pfeifer (Leipzig), and Professor Michel (Leipzig) for fruitful discussions. The authors gratefully acknowledge financial support from the Deutsche Forschungsgemeinschaft given in the frame of the SFB 294. S.M.A. gratefully acknowledges funding from the National Science Foundation (Grant No. CTS-9734153), a Sloan Foundation Research Fellowship (Grant No. BR-3844), and a Camille Dreyfus Teacher–Scholar Award (Contract No. TC-99-041).

[1] C. Baerlocher, W. M. Meier, and D. H. Olson, *Atlas of Zeolite Framework Types*, 5th rev. ed. (Elsevier, Amsterdam, 2001).
[2] *Proceedings of the 13th International Zeolite Conference*, edited by A. Galarneau, F. Di Renzo, F. Fajula, and J. Vedrine, Montpellier 2001 (Elsevier, Amsterdam, 2001).
[3] J. Kärger and D. M. Ruthven, *Diffusion in Zeolites and Other Microporous Solids* (Wiley, New York, 1992).
[4] S. M. Auerbach, Int. Rev. Phys. Chem. **19**, 155 (2000).
[5] C. Blanco, C. Saravanan, M. Allen, and S. M. Auerbach, J. Chem. Phys. **113**, 9778 (2000).
[6] M. P. Allen and D. Tildesley, *Computer Simulation of Liquids* (Clarendon Press, Oxford, 1989).
[7] W. Jorgensen, J. Madura, and C. Swenson, J. Am. Chem. Soc. **106**, 6638 (1984).
[8] P. Demontis, G. B. Suffritti, and A. Tilocca, J. Chem. Phys. **105**, 5586 (1996).
[9] P. Demontis, G. B. Suffritti, S. Quartieri, E. S. Fois, and A. Gamba, Zeolites **7**, 522 (1987).
[10] P. Demontis, G. B. Suffritti, S. Quartieri, E. S. Fois, and A. Gamba, J. Phys. Chem. **92**, 867 (1988).
[11] V. Gramlich and W. M. Meier, Z. Kristallogr. **133**, 134 (1971).
[12] S. Fritzsche, R. Haberlandt, J. Kärger, H. Pfeifer, and K. Heinzinger, Chem. Phys. **174**, 229 (1993).
[13] S. Fritzsche, R. Haberlandt, J. Kärger, H. Pfeifer, and K. Heinzinger, Chem. Phys. Lett. **198**, 283 (1992).
[14] S. Yashonath and P. Santikary, J. Phys. Chem. **97**, 13778 (1993).
[15] S. Bandyopadhyay and S. Yashonath, Chem. Phys. Lett. **223**, 363 (1994).
[16] S. Yashonath and C. Rajappa, Faraday Discuss. **106**, 105 (1997).